USCAP

www.nature.com/labinvest

ARTICLE

Check for updates

Nesfatin-1 exerts protective effects on acidosis-stimulated chondrocytes and rats with adjuvant-induced arthritis by inhibiting ASIC1a expression

Yayun Xu[1,2,3,4], Zhuoyan Zai[2,3,4], Tao Zhang[2,3], Longfei Wang[2,3], Xuewen Qian[2,3], Dandan Xu[2,3], Jingjing Tao[2,3], Zheng Lu[2,3], Zhengyu Zhang[2,3], Xiaoqing Peng[2,3] and Feihu Chen[1,2,3]✉

Nesfatin-1, a newly identified energy-regulating peptide, has been reported to possess antioxidant, anti-inflammatory, and antiapoptotic properties; however, to date, its effect on rheumatoid arthritis (RA) has not been previously explored in detail. We previously showed that activation of acid-sensing ion channel 1a (ASIC1a) by acidosis plays an important role in RA pathogenesis. Therefore, in this study, we evaluated the effects of nesfatin-1 on acidosis-stimulated chondrocyte injury in vitro and in vivo and examined the involvement of ASIC1a and the mechanism underlying the effects of nesfatin-1 on RA. Acid-stimulated articular chondrocytes were used to examine one of the several possible mechanisms underlying RA pathogenesis in vitro. The mRNA expression profile of acid-induced chondrocytes treated or not treated with nesfatin-1 was investigated by RNA sequencing. The effects of nesfatin-1 on oxidative stress, inflammation, and apoptosis in acid-induced chondrocytes were measured. The mechanistic effect of nesfatin-1 on ASIC1a expression and intracellular Ca^{2+} in acid-stimulated chondrocytes was studied. Rats with adjuvant-induced arthritis (AA) were used for in vivo analysis of RA pathophysiology. Cartilage degradation and ASIC1a expression in chondrocytes were detected in rats with AA after intraarticular nesfatin-1 injection. The in vitro experiments showed that nesfatin-1 decreased acidosis-induced cytotoxicity and elevation of intracellular Ca^{2+} levels in chondrocytes. Moreover, it attenuated acid-induced oxidative stress, inflammation, and apoptosis in chondrocytes. Nesfatin-1 decreased ASIC1a protein levels in acid-stimulated chondrocytes via the mitogen-activated protein kinase (MAPK)/extracellular signal-regulated kinase (ERK) and nuclear factor kappa-B (NF-κB) signaling pathways. In vivo analysis showed that nesfatin-1 ameliorated cartilage degradation and decreased ASIC1a expression in the chondrocytes of rats with AA. Collectively, nesfatin-1 suppressed acidosis-induced oxidative stress, inflammation, and apoptosis in acid-stimulated chondrocytes and alleviated arthritis symptoms in rats with AA, and its mechanism may be related to its ability to decrease ASIC1a protein levels via the MAPK/ERK and NF-κB pathways.

Laboratory Investigation (2022) 102:859–871; https://doi.org/10.1038/s41374-022-00774-y

INTRODUCTION

Rheumatoid arthritis (RA) is a chronic systemic autoimmune disease that affects ~1% of the global population[1]. Synovial cell proliferation and migration, inflammatory cell infiltration, pannus formation, and cartilage and bone destruction are the pathological hallmarks of RA[2]. Conventional treatments for RA include use of nonsteroidal anti-inflammatory drugs, corticosteroids, disease-modifying antirheumatic drugs (DMARD), and tumor necrosis factor (TNF) antagonists, which have a common anti-inflammatory mechanism[3]. The use of these drugs is mainly aimed at controlling synovial inflammation, rather than preventing cartilage destruction. Numerous studies have indicated that joint damage is not always associated with synovitis symptoms[4]. Articular cartilage destruction and loss reportedly continue even if joint inflammation is successfully suppressed[5,6]. Taken together, articular cartilage destruction and degeneration are the main reasons for loss of joint function[7]. Thus, developing new treatment strategies and identifying targets that would help control articular cartilage destruction to reduce the rate of joint dysfunction and disability would have great clinical significance.

Nesfatin-1, an energy-regulating peptide derived from the precursor protein nucleobindin-2 (NUCB2)[8], was recently reported to display potent anti-inflammatory, antiapoptotic, and antioxidative properties[9]. Nesfatin-1 has been found to inhibit reactive oxygen species (ROS) overproduction and reduce apoptosis in PC12 cells following high-glucose exposure[10]. Nesfatin-1 was also found to confer a significant cardioprotection against myocardial infarction by reducing pro-inflammatory cytokine levels[11]. More recently, it was shown to inhibit inflammation and reduce apoptosis in interleukin (IL)-1β-stimulated chondrocytes[12]. However, the antioxidant, anti-inflammatory, and antiapoptotic effects of nesfatin-1 on chondrocytes in RA and the molecular mechanism underlying its effects remain unclear.

[1]Department of Epidemiology and Biostatistics, School of Public Health, Anhui Medical University, Hefei, China. [2]Inflammation and Immune Mediated Diseases Laboratory of Anhui Province, Anhui Institute of Innovative Drugs, School of Pharmacy, Anhui Medical University, Hefei, China. [3]The Key Laboratory of Anti-inflammatory and Immune Medicines, Ministry of Education, Hefei, China. [4]These authors contributed equally: Yayun Xu, Zhuoyan Zai. ✉email: chenfeihu@ahmu.edu.cn

Received: 18 June 2021 Revised: 14 February 2022 Accepted: 15 February 2022
Published online: 15 March 2022

Acid-sensitive ion channel 1a (ASIC1a) is a member of the degenerin/epithelial sodium channel protein superfamily, which is transiently activated by extracellular acidification, and plays a critical role in various pathological processes, including RA[13,14]. Synovial fluid (SF) pH decreases in patients with RA[15–17] and in rats with adjuvant arthritis (AA)[18], an animal model widely used to mimic human RA. Moreover, joint fluid acidification has been reported to be associated with radiological joint destruction in patients with RA[17]. Our previous studies showed that ASIC1a is expressed in rat articular chondrocytes[19] and that extracellular acidosis increases ASIC1a protein levels in chondrocytes in a pH- and time-dependent manner[20]. Our research also indicated that ASIC1a is involved in articular chondrocyte injury induced by extracellular acidification, which could be attenuated by amiloride and the ASIC1a-specific blocker psalmotoxin 1 (PcTx1)[21,22]. Furthermore, synovial invasion and cartilage destruction were found to be ameliorated in rats that had AA and received PcTx1 joint injection[23,24]. Taken together, these findings indicate that the ASIC1a in chondrocytes is a potential therapeutic target for RA.

Accumulating evidence has indicated that inhibition of the nuclear factor kappa-B (NF-κB) signaling pathway may be involved in the mechanism underlying the anti-inflammatory, antiapoptotic, and antioxidative effects of nesfatin-1[25–27]. Therefore, our recent studies focused on determining the relationship between the NF-κB signaling pathway and ASIC1a expression in articular chondrocytes[18,28,29]. We found that pro-inflammatory cytokines, including IL-6, IL-1β, and TNF-α, induced ASIC1a expression in articular chondrocytes, mainly via the NF-κB signaling pathway[18,28]. Moreover, this signaling pathway was also found to be involved in the regulation of ASIC1a expression by nerve growth factor (NGF) and protein kinase C in chondrocytes[29,30]. The therapeutic potential of ASIC1a in RA indicates that nesfatin-1 may elicit protective response against RA by affecting ASIC1a expression via the NF-κB signaling pathway.

Therefore, in the current study, we aimed to investigate the protective effect of nesfatin-1 on RA because of its antioxidant, anti-inflammatory, and antiapoptotic properties and to elucidate the mechanism underlying its effects.

MATERIALS AND METHODS

Reagents

Nesfatin-1, PcTx1, and methotrexate (MTX) were purchased from Peprotech (Rocky Hill, NJ, USA), Abcam (Cambridge, MA, USA), and Shanghai Pharmaceutical (Group) Co., Ltd. (Shanghai, China), respectively. Antibodies against ASIC1a were purchased from Affinity Biosciences (OH, USA). Antibodies against caspase-9, cleaved caspase-9, poly ADP-ribose polymerase (PARP), cleaved PARP, ERK1/2, phospho-ERK1/2, Na^+-K^+-ATPase, nuclear factor of kappa light polypeptide gene enhancer in B-cells inhibitor (IκB) α, and ubiquitin (P4D1) were obtained from Cell Signaling Technology (Beverly, MA, USA). Antibodies against IL-6, IL-1β, TNF-α, Bax, Bcl-2, phospho-P65, P65, histone H3, and β-actin were obtained from Bioworld Technology Co., Ltd. (Nanjing, China). Antibodies against type II collagen (COL2A1) were obtained from Boster Biological Technology (Wuhan, China).

Animals

The study included 112 male Sprague-Dawley rats (weight range, 160–180 g) provided by the Experimental Animal Center of Anhui Medical University, Hefei, China. The rats were housed under controlled conditions (22 ± 2 °C and 12-h light/dark cycle) and allowed free access to standard pelleted food and water. All the animal experiments in this study were performed in strict accordance with the guidelines of the University Animal Care and Use Committee and were approved by the Ethics Committee of Anhui Medical University. An outline of the experimental design is shown in Supplementary Fig. S4A.

AA induction and treatment

AA was initiated in the rats by intradermal immunization in the right hind metatarsal footpad with 0.1 ml heat-killed mycobacteria (10 mg/ml) suspended in complete Freund's adjuvant (CFA; Chondrex Inc., Redmond, WA, USA). The rats were randomly divided into the following six groups ($n = 10$ per group): control, model, nesfatin-1 (10, 20, and 40 ng/ml), PcTx1 (8 μg/ml), and methotrexate (MTX; a DMARD; 0.5 mg/kg).

After the onset of arthritis on Day 21, the following treatment protocol was followed: the nesfatin-1 (10, 20, and 40 ng/ml) group rats were intraarticularly administered nesfatin-1 (50 μl solution) at the corresponding dose every 3 days; the PcTx1 group rats were intraarticularly administered PcTx1 (50 μl solution) at a 8 μg/ml dose every 3 days; the MTX group rats were intragastrically administered MTX at a 0.5 mg/kg dose every 3 days; and the control and model group rats were intraarticularly administered phosphate-buffered saline (PBS; 50 μl solution) every 3 days.

Clinical assessment of AA

The clinical parameters, that is, body weight, paw swelling, and polyarthritis index, of rats with AA, were evaluated every 3 days from Day 15 after induction. To assess paw swelling, the left hind paw volume was first determined using a YLS-TA volume meter (Shandong Academy of Medical Sciences Co., Ltd., Shandong, China) as the baseline paw volume before CFA injections. The hind paw volume was then measured at 3-day intervals following drug administration. Paw swelling has been expressed in terms of an increase in paw volume (ml), calculated by subtracting the baseline volume. For the polyarthritis index, arthritic severity was evaluated using the following macroscopic scoring system: 0, paws with no swelling or focal redness, 1 = paws with swelling of finger joints, 2 = paws with mild swelling of the ankle or wrist joints, 3 = paws with severe inflammation of the entire paw, and 4 = paws with deformity or ankylosis. The cumulative score for all four paws of each rat was used to represent the polyarthritis index score, with a maximum value of 16.

Immunohistochemical analysis and hematoxylin-eosin (HE) staining

The rats were anesthetized and sacrificed on Day 31 after the initial immunization, and the secondary ankle joints were harvested and fixed in 4% paraformaldehyde for 48 h, decalcified in 10% ethylenediaminetetraacetic acid (EDTA) for 4 weeks, and embedded in paraffin. Subsequently, serial sections (4 μm) were cut. Immunohistochemical analysis was performed with SP-9000 Histostain-Plus kits (ZSGB Bio, China) according to the manufacturer's instructions. HE (Beyotime, Beijing, China) staining was performed according to the manufacturer's protocol. The samples were visualized using a digital pathology slide scanner (3DHISTECH; The Digital Pathology Company, Budapest, Hungary). The Image-ProPlus software (Media Cybernetics, Silver Spring, MD, USA) was used to calculate the integral optical density (IOD) of the immunohistochemical sections.

Isolation of articular chondrocytes and treatment

Primary articular chondrocytes were extracted from rats by using a previously described method[18]. Briefly, cartilage from the knee joint was minced into small pieces (~ 1 mm^3) and initially digested using 0.25% trypsin for 30 min at 37 °C. Subsequently, the samples were washed thrice with PBS and treated with 0.2% type II collagenase (Sigma Aldrich, USA) in PBS for 6 h at 37 °C. After the digestion procedure, the isolated cells were centrifuged at 200 × g for 10 min and washed thrice with PBS. The freshly isolated chondrocytes were plated at a density of 2×10^4 cells/well, following immersion in plastic dishes filled with Dulbecco's Modified Eagle Medium (DMEM)/F-12 (HyClone Laboratories, Logan, UT, USA) supplemented with 10% fetal bovine serum (BI, Jerusalem, Israel), 100 IU/ml penicillin, and 100 μg/ml streptomycin. The cells were maintained under sterile conditions at 37 °C in a humidified 5% CO_2 incubator.

Immunocytochemical analysis of COL2A1 and toluidine blue staining of glycosaminoglycan for characterizing articular chondrocytes

Immunocytochemical analysis of COL2A1 and toluidine blue staining of glycosaminoglycan were used to characterize the isolated articular chondrocytes. For immunocytochemical analysis of COL2A1, articular chondrocytes were seeded in six-well plates at 4×10^4 cells per well and allowed to grow to ~70–80% confluence. After the cells were washed thrice with PBS, they were fixed with 4% paraformaldehyde at room temperature for 15 min. The cells were then permeabilized for 10 min with 0.1% Triton X-100 and blocked with 3% bovine serum albumin (BSA) for 1 h. Subsequently, they were incubated with anti-COL2A1 antibody (1:200 dilution; Boster Biological Technology) overnight at 4 °C and fluorescein

Table 1. Primer sequences for real-time PCR.

Gene	Forward primer	Reverse primer
ASIC1a	5′-GAGAAGCACAAGGAGATGACACG-3′	5′-AGACAAAGGGCACCAGGATAGG-3′
β-actin	5′-CCCATCTATGAGGGTTACGC-3′	5′-TTTAATGTCACGCACGATTTC-3′
IL-1β	5′-CTCAACTGTGAAATAGCAGCTTTC-3′	5′-GGACAGCCCAAGTCAAGG–3′
IL-6	5′-GAGCCCACCAGGAACGAAAGTC-3′	5′-TGTTGTGGGTGGTATCCTCTGTGAA-3′
TNF-α	5′-ACTCCCAGAAAAGCAAGCAA-3′	5′-CAGTTCCACATCTCGGATCA-3′

isothiocyanate (FITC)-conjugated anti-rat IgG (Bioss, Beijing, China) for 1 h at 37 °C. Next, the cells were washed thrice with PBS, following which they were stained for 10 min with 3-3′-diaminobenzidine (DAB) and counterstained with 0.1% hematoxylin for nuclear staining for 30 s.

For toluidine blue staining of glycosaminoglycan, the cells were washed thrice with PBS and fixed with 4% paraformaldehyde at room temperature for 15 min. Then, they were stained with 1% toluidine blue for 5 min and washed with water. Image processing was performed using an inverted fluorescence microscope (Olympus, Tokyo, Japan).

3-(4,5-Dimethylthiazol-2-yl)-2,5-diphenyltetrazolium bromide (MTT) assay

Articular chondrocytes were plated in 96-well plates overnight and then incubated with fresh medium containing nesfatin-1, PcTx1, or vehicle for various durations. After the treatments, 20 μl MTT solution (5 mg/ml; Sigma-Aldrich, St Louis, MO, USA) was added to each well, and the plates were incubated at 37 °C in 5% CO_2 for 4 h. After the supernatant was removed, the cells were treated with 150 μl dimethyl sulfoxide (DMSO; Sigma-Aldrich) at 37 °C for 10 min to dissolve the formazan crystals. Optical density (OD) was measured using a microplate reader (Multiskan MK3; Thermo, USA) at a wavelength of 492 nm.

Quantitative real-time (qRT)-polymerase chain reaction (PCR)

Total RNA was extracted from articular chondrocytes by using TRIzol Reagent (Invitrogen, Carlsbad, CA, USA) according to the manufacturer's instructions and then reverse transcribed into complementary DNA (cDNA) by using a First Strand cDNA Synthesis Kit (Thermo Fisher Scientific, Waltham, MA, USA). The cDNAs synthesized were utilized for qRT-PCR, which was performed using a CFX96 Real-time RT-PCR detection system (Bio-Rad, USA) and a SYBR Premix Ex Taq kit (TaKaRa Biotechnology, Tokyo, Japan) in a 25 μl volume for 40 cycles (15 s at 95 °C, 60 s at 62 °C, and 72 °C for 30 s). The primer sequences used are shown in Table 1. The Ct values of the samples were calculated and the transcript levels were analyzed using the $2^{-\Delta\Delta Ct}$ method.

RNA sequencing and data analysis

RNA concentration and purity were measured using a NanoDrop Spectrophotometer (Thermo Fisher, USA) and a Labchip GX Touch HT Nucleic Acid Analyzer (PerkinElmer, USA). High-quality RNA samples were sent to the WuHan Bioacme Biological Technologies Corporation (Wuhan, China) for cDNA library construction and sequencing. Total mRNA was enriched and purified using oligo (dT)-containing magnetic beads. RNA sequencing libraries were generated using the KAPA Stranded RNA-Seq Kit (KAPA Biosystems, Wilmington, USA) for Illumina with multiplexing primers, according to the manufacturer's protocol. All the samples were sequenced using an Illumina Nova sequencer.

Differential expression analysis of two conditions/groups (three biological replicates per condition) was performed using the DESeq R package (1.10.1). DESeq provides statistical routines for determining differential expression based on digital gene expression data using a model based on negative binomial distribution. The resulting *P*-values were adjusted using Benjamini and Hochberg's approach for controlling the false discovery rate. Genes with an adjusted *P*-value of <0.05, identified by DESeq, were assigned as differentially expressed.

Kyoto Encyclopedia of Genes and Genomes (KEGG, https://www.genome.jp/kegg/pathway.html) pathway analysis was performed to investigate the pathways enriched by the differentially expressed genes.

Western blot analysis

Western blot analysis was performed to evaluate protein levels. Briefly, cells were washed twice with ice-cold PBS and lysed in radioimmunoprecipitation assay (RIPA) buffer containing protease inhibitors and protein phosphatase inhibitors. Protein concentrations were measured using a BCA Protein Assay Kit (Beyotime Biotechnology). Equal amounts of protein samples from each group were separated by 10% sodium dodecyl sulfate (SDS)-polyacrylamide gel electrophoresis (PAGE) and transferred onto polyvinylidene difluoride (PVDF) membranes (Millipore Corp). Then, the membranes were blocked with 5% nonfat milk in Tris-buffered saline containing 0.1% Tween-20 (TBST) at room temperature for 2 h and incubated with specific primary antibodies against ASIC1a, IL-6, IL-1β, TNF-α, Bax, Bcl-2, cleaved caspase-9, caspase-9, cleaved-PARP, PARP, phospho-P65, P65, phospho-ERK1/2, ERK1/2, IκBα, ubiquitin, Na^+-K^+-ATPase, histone H3, and β-actin (1:1000) at 4 °C overnight. The membranes were then washed thrice with TBST and incubated with horseradish peroxidase (HRP)-conjugated secondary antibodies (1:10,000 dilution) for 1 h. The protein bands were detected using the ECL chemiluminescent kit (Thermo Fisher Scientific) and analyzed using the ImageJ software. In addition, positive and negative controls were included to confirm the specificity of the anti-ASIC1a antibody according to the Abcam official website (https://www.abcam.cn/asic1-antibody-epr25411-45-ab284406.html; Supplementary Fig. S1A). Rat brain and kidney tissue lysates were used for the positive and negative controls, respectively. Antibody binding specificity was also examined using the respective blocking peptides (catalog number: DF9198-BP; Affinity Biosciences, OH, 161, USA).

Oxidative stress marker (ROS, malondialdehyde [MDA], and glutathione [GSH]) analyses

Intracellular ROS levels were measured using the ROS-sensitive fluorescent dye 2′,7′-dichlorofluorescein diacetate (DCFH-DA) (Beyotime Biotechnology), as previously described[31]. Briefly, cells were washed twice with PBS and incubated with 10 μmol/L DCFH-DA for 20 min at 37 °C. They were then washed thrice with serum-free DMEM/F-12 and photographed under a fluorescence microscope (Olympus) at excitation and emission wavelengths of 488 and 525 nm, respectively. Cellular MDA and GSH levels were analyzed using a commercial kit (Jiancheng Co., Nanjing, China) according to the manufacturer's instructions.

Immunofluorescence staining

Cultured cells were washed twice with PBS and fixed in 4% paraformaldehyde for 15 min at room temperature. The cells were then permeabilized for 10 min with 0.1% Triton X-100 and blocked with 3% BSA for 1 h. Subsequently, the cells were stained with anti-ASIC1a or anti-NF-κB P65 antibodies (Bioss, Beijing, China) overnight at 4 °C. Next, they were washed thrice for 5 min with PBS and were then incubated with the corresponding fluorescent-labeled secondary antibody (FITC-labeled goat anti-rabbit IgG; Wuhan Boster Co.) for 1 h at 4 °C in the dark and then counterstained with 4′,6-diamidino-2-phenylindole (DAPI) for 5 min. Images were captured using a fluorescence inversion microscopesystem (Olympus). In addition, positive and negative controls for the anti-ASIC1a antibody were included to confirm its specificity according to the Abcam official website (https://www.abcam.cn/asic1-antibody-ab236770.html; Supplementary Fig. S1B). HepG2 cells (human liver carcinoma cell line) and HT22 cells (hippocampal neuronal cell line) were used as positive controls, and 293 T cells (human embryonic kidney cell line) were used as the negative control. The ASIC1a protein was found to be mainly located in the cytoplasm.

Cytokine analysis

Primary articular chondrocytes were pre-incubated as previously described. The cell culture media were collected and centrifuged at 1000 × *g* for 20 min to remove cell debris and impurities. Blood samples were obtained from the abdominal aorta of the rats and were immediately centrifuged at 1000 × *g* for 5 min at 4 °C. Serum was obtained as the supernatant. The extracted culture media and sera were stored at −80 °C until analysis. Commercially available enzyme-linked immunosorbent assay (ELISA) kits were used to measure the

IL-6, IL-17, IL-1β, and TNF-α concentrations (Jianglai Bio, Shanghai, China) according to the manufacturer's instructions.

Co-immunoprecipitation (Co-IP)

Cells were lysed in cell lysis buffer (Biosense Bioscience Co., Ltd., Guangzhou, China) supplemented with a protease inhibitor cocktail. For immunoprecipitation, cell lysates were incubated under shaking conditions with anti-IκBα or rabbit IgG antibodies (Cell Signaling Technology, MA, USA) overnight at 4 °C; subsequently, protein A/G agarose beads were added and the mixture was incubated for 4 h. The beads were then washed thrice with lysis buffer. Subsequently, the immunoprecipitated complexes were analyzed by western blotting.

Membrane and nuclear protein extracts

Cell membrane proteins were extracted from a cell suspension (5×10^7 cells) by using a membrane protein extraction kit (Beyotime Biotechnology) according to the manufacturer's instructions. Cell nuclear proteins were extracted from the cell suspension (5×10^7 cells) by using a nuclear protein extraction kit (KeyGEN, China) according to the manufacturer's instructions.

Fluorescence microscopy and flow cytometry analyses of intracellular calcium concentration

For fluorescence microscopy, the cells were washed thrice with D-Hanks' solution and incubated with 5 μM Fluo 3-AM (Dojindo Laboratories, Japan) for 30 min in the dark at 37 °C. Next, they were washed thrice with D-Hanks' solution and then incubated with fresh D-Hanks' solution for 10 min in the dark at 37 °C. Fluo 3-AM was excited at 488 nm, and emission was measured at 510 nm.

For flow cytometry, the cell suspensions were washed thrice with D-Hanks' solution and incubated with 5 μM Fluo 3-AM for 30 min in the dark at 37 °C. Next, the cells were washed thrice for 5 min and incubated in D-Hanks' solution for 10 min in the dark at 37 °C. The cells were detected using a flow cytometer (Beckman Coulter, USA), and the images were analyzed using the CytoExpert software (Beckman Coulter) to determine fluorescence intensity.

Apoptosis analysis

For terminal deoxynucleotidyl transferase dUTP nick end labeling (TUNEL) staining, the cells were washed twice with PBS after the various treatments and then stained with TUNEL staining reagent (Beyotime Biotechnology) according to the manufacturer's instructions. Fluorescence images were captured using a fluorescent microscope. The apoptosis rate was quantified by counting TUNEL-positive cells from five random fields of view.

For flow cytometry, the cells were harvested, washed twice with cold PBS, and incubated with an Annexin V-FITC (5 μl) solution for 15 min, followed by incubation with propidium iodide (PI; 10 μl; Bioworld Technology, Co., Ltd.) for 10 min in the dark at 4 °C. The cells were detected using a flow cytometer, and the images were analyzed using the CytoExpert software to determine the apoptotic ratio.

Statistical analysis

All statistical analyses were performed using SPSS (Statistical Package for the Social Sciences) version 17.0.1 (SPSS Inc., Chicago, IL, USA). Data have been expressed in terms of the mean ± standard error of the mean (SEM) values, and statistical significance was set at $P < 0.05$. Between-group effects on body weight, paw swelling, and polyarthritis index were analyzed using repeated-measures analysis of variance (ANOVA) followed by the least significant difference (LSD) test. Student's *t* test for independent samples was used for comparisons between two groups. One-way ANOVA, followed by the LSD post-hoc test, was performed for three or more groups.

RESULTS

Nesfatin-1 attenuated acidosis-induced cytotoxicity and decreased ASIC1a protein levels in articular chondrocytes

Primary articular chondrocytes were identified based on the expression of articular chondrocyte markers via immunocytochemical staining of COL2A1 (Supplementary Fig. S2A) and toluidine blue staining of glycosaminoglycan (Supplementary Fig. S2B). To determine whether nesfatin-1 affected acidosis-induced injury, we first examined acid-induced toxicity in cultured articular chondrocytes with and without nesfatin-1 pretreatment. The MTT assay showed that cell viability was not affected by nesfatin-1 treatment alone (24 h), at concentrations ranging from 5 to 80 ng/ml (Supplementary Fig. S2C). Compared with the control group, 3-h acid incubation (pH 6.0) decreased cell viability (Fig. 1A). Pretreatment with nesfatin-1 (10–80 ng/ml, 24 h)

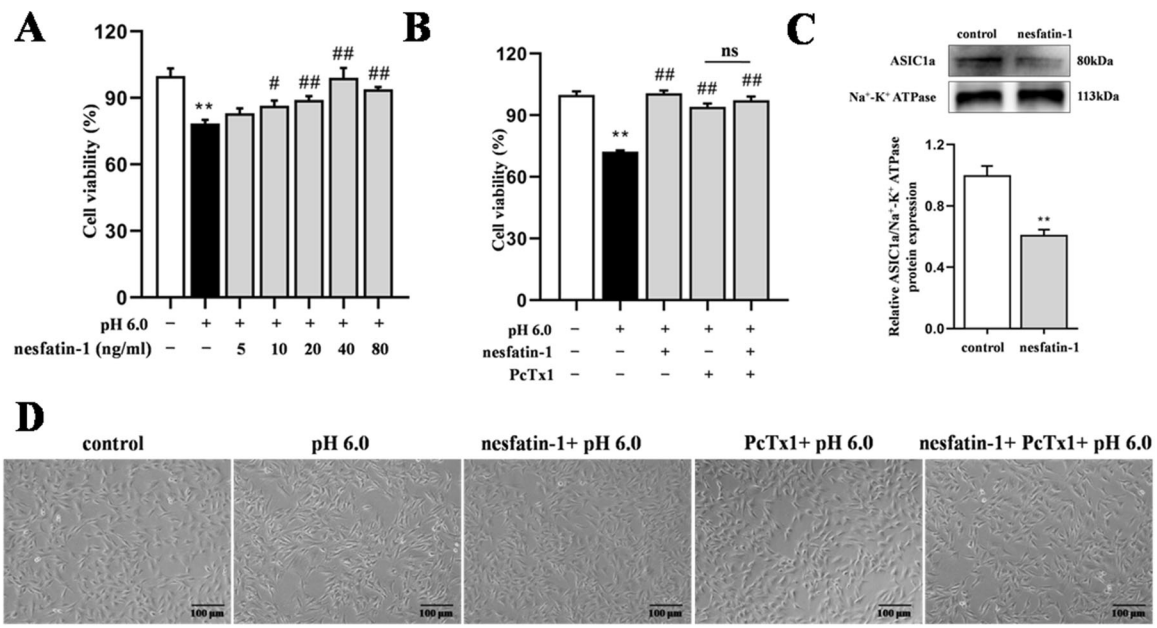

Fig. 1 Nesfatin-1 attenuated acidosis-induced cytotoxicity in primary rat articular chondrocyte. A Nesfatin-1 restored cell viability in acidosis-induced articular chondrocytes, which was determined using the MTT assay. **B** Cell viability was assessed with the MTT assay in acid-stimulated chondrocytes after nesfatin-1 and PcTx1 pretreatment. **C** Membrane ASIC1a protein was detected by western blotting in articular chondrocytes, with or without nesfatin-1 treatment. **D** Representative phase-contrast images showing chondrocytes, which were obtained after treatment with the indicated solutions. Data represent the mean ± SEM values for three independent experiments. $^{**}P < 0.01$ compared to the control group; $^{\#}P < 0.05$, $^{\#\#}P < 0.01$ compared to the pH 6.0 group; ns: no significance.

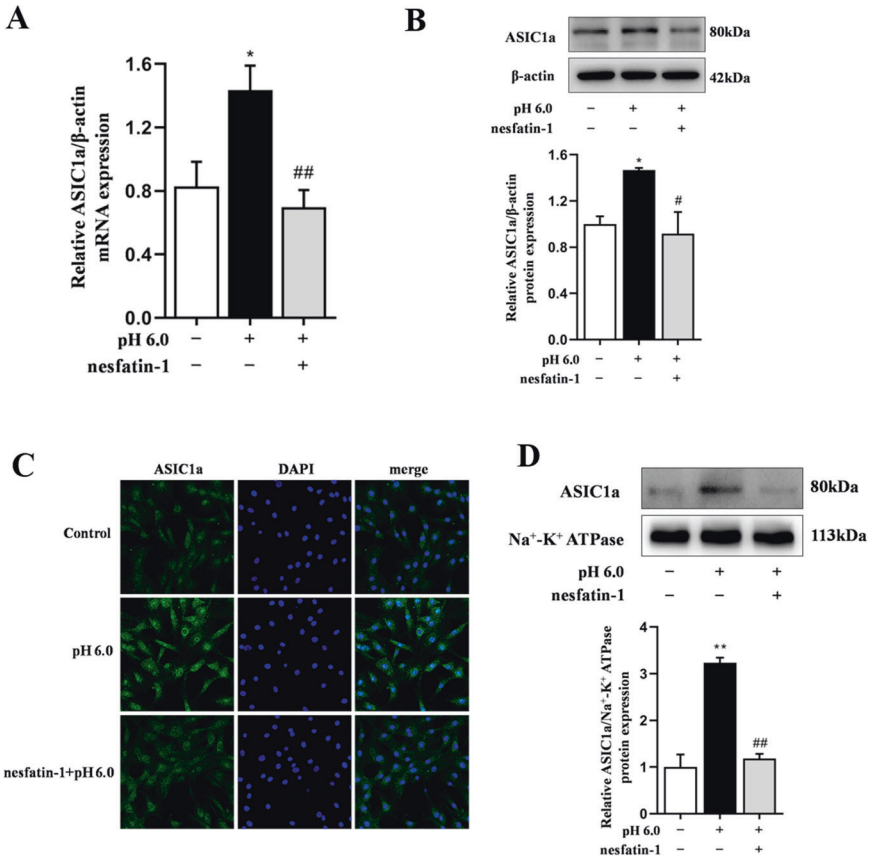

Fig. 2 Nesfatin-1 downregulated ASIC1a expression in articular chondrocytes and decreased the upregulation of ASIC1a expression induced by acidosis in articular chondrocytes. A ASIC1a mRNA levels in acid-mediated chondrocytes were measured after nesfatin-1 pretreatment by using real time-PCR. **B** ASIC1a protein levels in acid-mediated chondrocytes were measured after nesfatin-1 pretreatment by using western blotting. **C** The effects of nesfatin-1 on the ASIC1a expression levels were analyzed by immunofluorescence. **D** Membrane ASIC1a protein was detected by western blotting in acid-stimulated articular chondrocytes, with or without nesfatin-1 treatment. Data represent the mean ± SEM values for three independent experiments. $^{*}P < 0.05$, $^{**}P < 0.01$ compared to the control group; $^{\#}P < 0.05$, $^{\#\#}P < 0.01$ compared to the pH 6.0 group.

attenuated the acidosis-induced decrease in cell viability (Fig. 1A). ASIC1a activation plays an important role in acidosis-induced chondrocyte injury. The addition of PcTx1 (100 nmol/L), an ASIC1a inhibitor, largely attenuated acidosis-induced cytotoxicity (Fig. 1B). However, combined treatment with nesfatin-1 and PcTx1 did not provide additional protection beyond that obtained with PcTx1 alone (Fig. 1B), suggesting that ASIC1a channel inhibition is likely involved in nesfatin-1-mediated protection. Consistent with this finding, acid exposure-induced cell body deformation was attenuated by nesfatin-1 or PcTx1 treatment (Fig. 1D).

To investigate whether the protective effect of nesfatin-1 was mediated by changes in ASIC1a protein levels, articular chondrocytes were treated with nesfatin-1 (5–40 ng/ml) or vehicle for 3–48 h, followed by measurement of ASIC1a mRNA and protein expression levels. Nesfatin-1 pretreatment (20, 40, and 80 ng/ml, 24 h; 40 ng/ml, 24–48 h) significantly decreased ASIC1a mRNA expression (Supplementary Fig. S2D, E). Similarly, nesfatin-1 pretreatment (40 and 80 ng/ml, 24 h; 40 ng/ml, 12, 24, and 48 h) significantly decreased ASIC1a protein levels (Supplementary Fig. S2F, G). On the basis of the MTT assay results, nesfatin-1 treatment performed using 40 ng/ml concentration for 24 h was selected for the subsequent experiments. Immunofluorescence staining of ASIC1a decreased in chondrocytes after nesfatin-1 pretreatment (Supplementary Fig. S2H). ASIC1a is a membrane proton receptor; therefore, the number of ASIC1a present on the cell surface determines its physiological and pathological functions[32]. The ASIC1a protein level on the cell membrane also decreased in the chondrocytes (38.9% reduction; Fig. 1C).

Nesfatin-1 decreased the increased ASIC1a protein levels in acid-stimulated chondrocytes

To further examine the effect of nesfatin-1 on ASIC1a expression in acid-stimulated chondrocytes, the acid-stimulated chondrocytes were treated with nesfatin-1, which was followed by measurement of ASIC1a protein levels. Nesfatin-1 pretreatment significantly downregulated the increased ASIC1a mRNA and protein expression induced by acid stimulation (Fig. 2A, B). Consistent with this finding, immunofluorescence staining also showed that the increased ASIC1a protein levels induced by acid stimulation were reduced by nesfatin-1 treatment (Fig. 2C). Acid stimulation increased membrane ASIC1a protein levels in chondrocytes, which was reversed by nesfatin-1 treatment (63.3% reduction; Fig. 2D). These results indicate that the protective effect of nesfatin-1 on acid-induced articular chondrocytes may be attributable to reduction of ASIC1a expression by nesfatin-1.

Nesfatin-1 treatment suppressed acid-induced $(Ca^{2+})i$ elevation

Ca^{2+} is considered to act as a crucial downstream mediator effector after ASIC1a channel activation;[33] ASIC1a contributes to acid-induced injury by increasing intracellular Ca^{2+} in rat articular chondrocytes[34]. Therefore, we analyzed whether nesfatin-1 affects acid-induced $(Ca^{2+})i$ elevation. Immunofluorescence staining

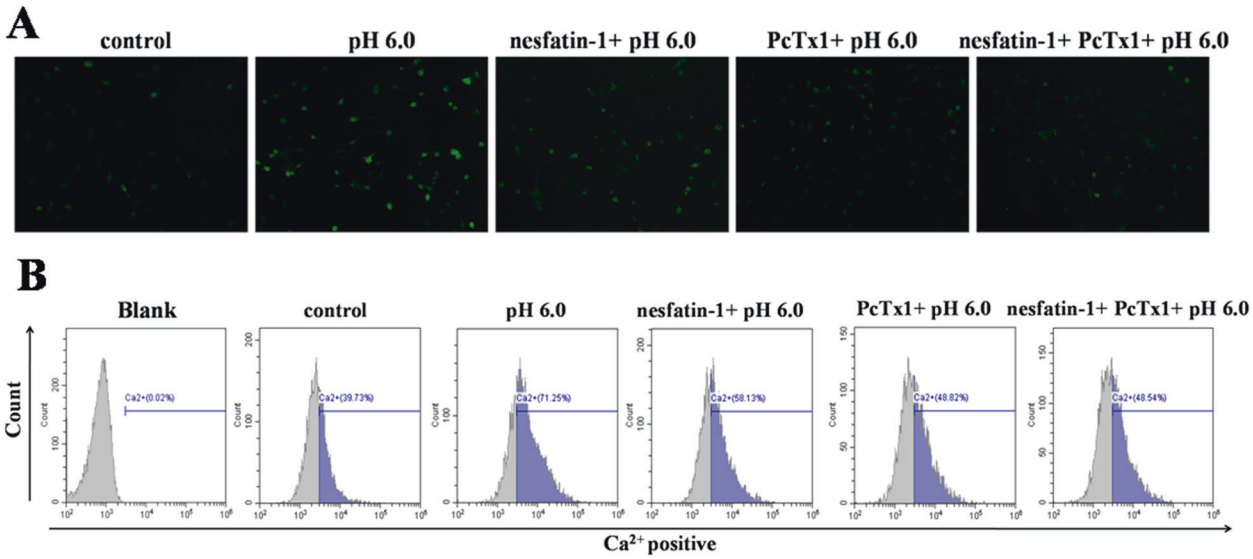

Fig. 3 Nesfatin-1 suppressed acid-induced $(Ca^{2+})i$ elevation in articular chondrocytes. A The effects of nesfatin-1 on the intracellular Ca^{2+} levels were analyzed by immunofluorescence. **B** The effects of nesfatin-1 on the intracellular Ca^{2+} levels were analyzed by flow cytometry.

(Fig. 3A) and flow cytometry (Fig. 3B) analyses revealed that nesfatin-1 treatment significantly suppressed the increase in $(Ca^{2+})i$ levels induced by extracellular acidification in chondrocytes, suggesting that ASIC1a-Ca^{2+} involved in the protective effect of nesfatin-1 on acidosis-induced injury.

Differential mRNA expression in acid-stimulated articular chondrocytes, with or without nesfatin-1 treatment

RNA sequencing was performed to determine the mRNA expression profiles of acid-induced chondrocytes that were treated or not treated with nesfatin-1. Differential mRNA expression was evaluated in the control, pH 6.0, and pH 6.0+nesfatin-1 groups via a heatmap of the gene expression patterns (Fig. 4A). Changes in mRNA expression among the three groups were determined using Venn diagrams (Fig. 4B). The Venn diagram shows that 1011 mRNAs were differentially co-expressed among the three groups. KEGG enrichment analyses indicated that differentially expressed mRNAs were involved in pathways related to oxidative stress, inflammation, and apoptosis, such as the TNF signaling pathway, MAPK signaling pathway, cytokine-cytokine receptor interaction, the apoptosis process, positive regulation of NF-κB transcription factor activity, and regulation of the ROS metabolic process (Fig. 4C, D).

Nesfatin-1 attenuated acid-induced oxidative stress, inflammation, and apoptosis in chondrocytes

On the basis of the RNA sequencing results, we further investigated the effect of nesfatin-1 on acidification-induced oxidative stress in articular chondrocytes. DCFH-DA staining showed that ROS generation increased in the acid-stimulated chondrocytes (Fig. 5A). However, ROS levels significantly decreased when acid-stimulated chondrocytes were treated with nesfatin-1 (Fig. 5A). Consistent with these findings, the MDA and GSH levels in the culture supernatant significantly increased and decreased, respectively, in chondrocytes after acid exposure, which was reversed by nesfatin-1 treatment (Fig. 5B, C).

Nesfatin-1 downregulated the increased IL-6, IL-1β, and TNF-α mRNA levels (Fig. 5D–F) and protein levels (Fig. 5G and Supplementary Fig. S3A–C) in acid-stimulated chondrocytes. Given that these pro-inflammatory cytokines are secretory proteins, their levels in the culture supernatant were also measured. The IL-6, IL-1β, and TNF-α levels in the culture supernatant significantly increased in chondrocytes after acid exposure and were decreased by nesfatin-1 treatment (Fig. 5H–J).

Annexin V-FITC/PI staining (Fig. 5K and Supplementary Fig. S3D) and TUNEL staining (Fig. 5L, M) showed that nesfatin-1 partly abrogated the increase in apoptosis due to acid stimulation. Western blotting showed that the Bax/β-actin, cleaved caspase-9/caspase-9, and cleaved-PARP/PARP expression levels increased, whereas the Bcl-2/β-actin expression levels decreased in the pH 6.0 group. These effects were reversed by nesfatin-1 treatment (Fig. 5N and Supplementary Fig. S3E–H).

Additionally, combined treatment with nesfatin-1 and PcTx1 did not provide additional effect on acid-induced oxidative stress, inflammation, and apoptosis beyond that obtained with PcTx1 alone (Fig. 5), further suggesting that that there is no synergy between nesfatin-1 and PcTx1, and inhibiting ASIC1a channel is likely involved in nesfatin-1-mediated protection.

Nesfatin-1 decreased ASIC1a expression via MAPK/ERK and NF-κB signaling

The KEGG enrichment results suggested that MAPK and NF-κB signaling is involved in the effect of nesfatin-1 on acid-stimulated articular chondrocytes. The p-ERK1/2/ERK1/2 and p-P65/P65 protein levels significantly increased in acid-stimulated articular chondrocytes (Fig. 6A–C), which were reduced by nesfatin-1 treatment.

To further investigate the potential role of nesfatin-1-induced inhibition of the MAPK/ERK and NF-κB pathways in the downregulation of ASIC1a expression in chondrocytes, the inhibitors PD098059 (specific pharmacological inhibitor of the ERK pathway) and PDTC (NF-κB-specific inhibitor) were used to block these signaling pathways. Both nesfatin-1 and PD098059 decreased ASIC1a protein levels (Fig. 6D). However, combined treatment with nesfatin-1 and PD098059 did not lead to additional decreases beyond those obtained with PD098059 alone, suggesting that MAPK/ERK signaling is likely involved in nesfatin-1-mediated inhibition of ASIC1a production. Similarly, both nesfatin-1 and PDTC decreased ASIC1a protein levels. However, combined treatment with nesfatin-1 and PDTC did not lead to additional decreases beyond those obtained with PDTC alone (Fig. 6E), suggesting that NF-κB signaling is likely involved in nesfatin-1-mediated inhibition of ASIC1a production.

In the canonical NF-κB pathway, NF-κB activation depends on IκBα degradation and nuclear translocation of P65. To confirm the role played by NF-κB in the regulation of ASIC1a expression by nesfatin-1 and the mechanism underlying this effect, we investigated the effect of nesfatin-1 on the degradation of ubiquitylated IκBα and the nuclear translocation of NF-κB P65 in acid-stimulated chondrocytes.

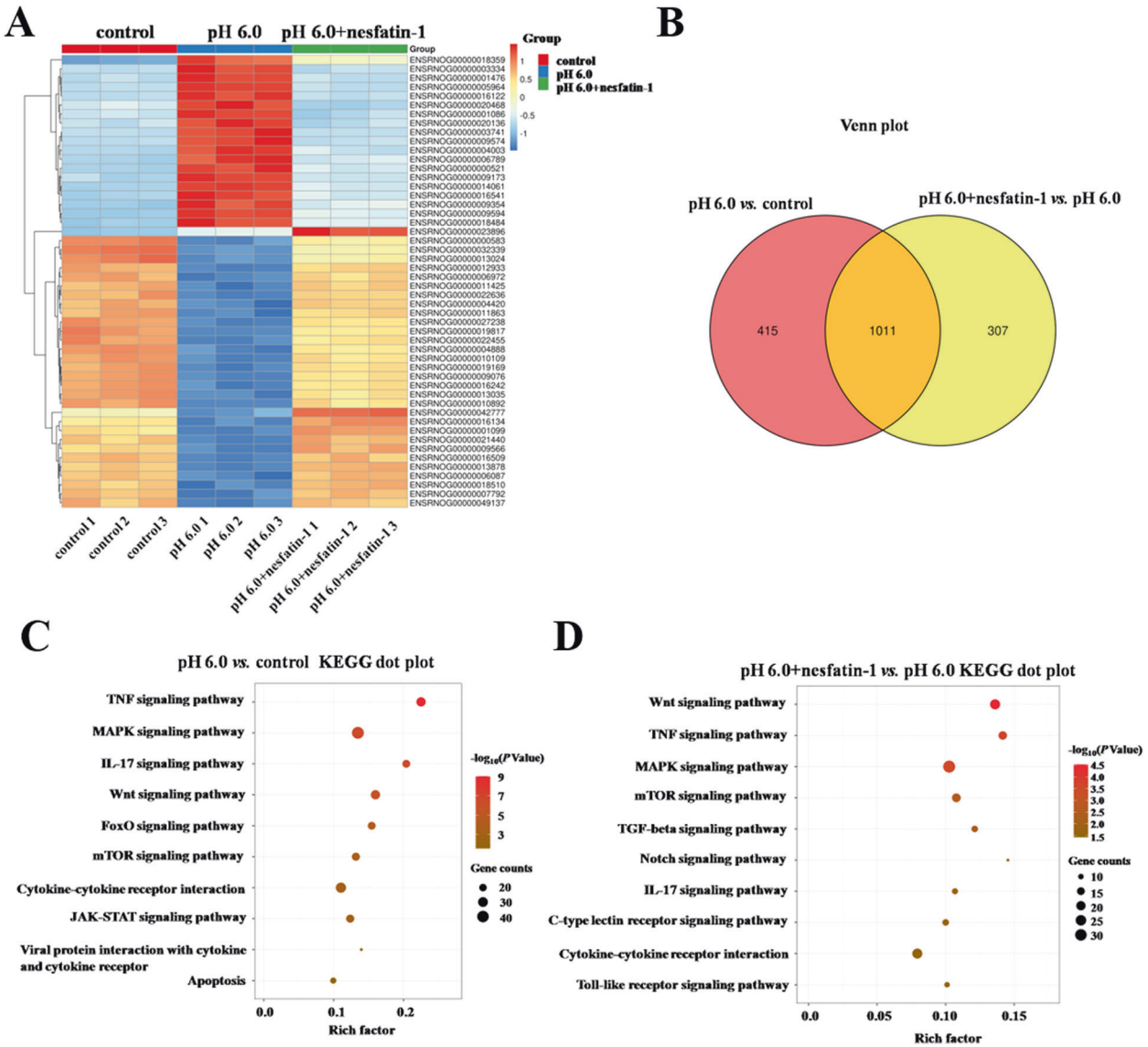

Fig. 4 mRNA expression profile changes in the control, pH 6.0, and pH 6.0+nesfatin-1 groups. A Heat map showing differentially expressed mRNAs with the same expression pattern in control and pH 6.0+nesfatin-1 groups, which was the opposite of that noted in the pH 6.0 group. **B** Venn diagram showing the number of overlapping mRNAs in the three groups. **C** KEGG enrichment analysis of co-differentially expressed genes in the control and pH 6.0 groups. **D** KEGG enrichment analysis of co-differentially expressed genes in the pH 6.0 and pH 6.0+nesfatin-1 groups.

The results of WB (Fig. 6F) and immunofluorescence staining (Fig. 6G) showed that the P65/histone H3 protein levels in the nucleus in the pH 6.0 group significantly increased, and nesfatin-1 treatment reversed this effect (Histone H3 was used as nuclear control protein). CO-IP analysis showed that the increase in ubiquitylated IκBα degradation in acid-stimulated chondrocytes was decreased by nesfatin-1 treatment (Fig. 6H). These data indicated that nesfatin-1 decreased the acid stimulation-induced upregulation of ASIC1a expression, mainly by inhibiting the degradation of ubiquitylated IκBα and nuclear translocation of NF-κB P65.

Nesfatin-1 attenuated clinical signs, improved ankle joint histopathological features, decreased serum inflammatory cytokine levels, and decreased ASIC1a levels in the chondrocytes of rats with AA

To investigate the protective role of nesfatin-1 in chondrocytes in vivo, the clinical signs and cartilage degradation in rats with AA were analyzed after intraarticular nesfatin-1 injection.

Repeated-measures ANOVA revealed that both treatment ($F = 5.173$, $P < 0.001$) and time ($F = 4.449$, $P = 0.014$) had a significant effect on body weight, with significant interaction ($F = 8.568$, $P < 0.001$). LSD analysis showed that the model rats had lower body weight than the control rats at 36 days; however, the body weight of the model group did not significantly differ from that of the other groups (Supplementary Fig. S4B).

Both treatment and time affected paw swelling (treatment effect: $F = 15.289$, $P < 0.001$; time effect: $F = 32.305$, $P < 0.001$; interactive effect: $F = 7.367$, $P < 0.001$). At 36 days, the paw swelling in the control and treatment groups was lower than that in the model group (Supplementary Fig. S4C).

Both treatment and time affected the polyarthritis index (treatment effect: $F = 6.374$, $P < 0.001$; time effect: $F = 28.404$, $P < 0.001$; interactive effect: $F = 9.558$, $P < 0.001$). At 36 days, the polyarthritis indexes of the treatment group were all lower than those of the model group (Fig. 7A). Consistent with this finding, the foot claw of the rats with AA showed obvious swelling

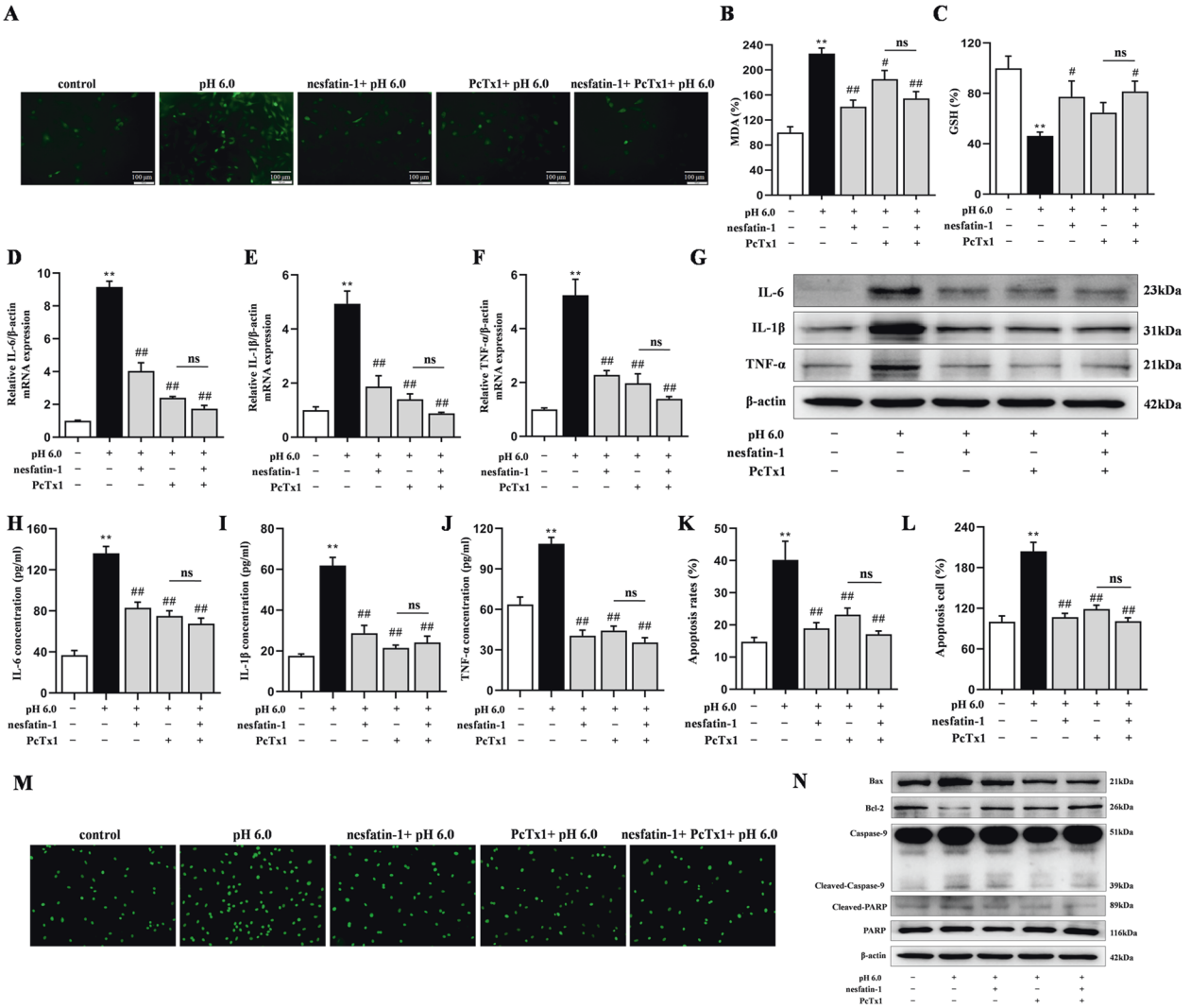

Fig. 5 Nesfatin-1 attenuated acid-induced oxidative stress, inflammation, and apoptosis in articular chondrocytes. A 2′,7′-dichlorofluorescin (DCF) staining of intracellular ROS. Nesfatin-1 reduced acid-induced ROS generation. **B** Effects of nesfatin-1 on acid-induced MDA levels. **C** Effects of nesfatin-1 on acid-induced GSH levels. **D**–**F** The mRNA levels of inflammatory cytokines (IL-6, IL-1β, and TNF-α) in acid-mediated chondrocytes after nesfatin-1 and PcTx1 pretreatment were measured using real time-PCR. **G** The IL-6, IL-1β, and TNF-α protein levels in acid-mediated chondrocytes after nesfatin-1 and PcTx1 pretreatment were measured using western blotting. **H**–**J** The IL-6, IL-1β, and TNF-α levels in the culture supernatant after nesfatin-1 and PcTx1 pretreatment were measured using ELISA. **K** Acid-induced chondrocyte apoptosis after nesfatin-1 and PcTx1 pretreatment was detected using the Annexin-V/PI assay. **L**, **M** Acid-induced chondrocyte apoptosis after nesfatin-1 and PcTx1 pretreatment was detected using the TUNEL assay. **N** Bax, Bcl-2, cleaved caspase-9/caspase-9, and cleaved-PARP/PARP protein levels were analyzed by western blotting. Data represent the mean ± SEM values for three independent experiments. $^{**}P < 0.01$ compared to the control group; $^{\#}P < 0.05$, $^{\#\#}P < 0.01$ compared to the pH 6.0 group; ns: no significance.

compared to the foot claw of the control rats; this swelling was alleviated in the nesfatin-1-treated groups (10, 20, and 40 ng/ml; Fig. 7B). The rats with AA developed severe arthritis, which was characterized by marked synovial proliferation, pannus formation, inflammatory cell infiltration, and articular cartilage and bone erosion (Fig. 7C, D). Nesfatin-1 protected the rats from bone erosion and joint destruction, and almost no articular cartilage erosion was observed in the groups that received nesfatin-1 (20 and 40 ng/ml), which was similar to the effect of PcTx1 and MTX.

The COL2A1 expression in the chondrocytes of the model group was significantly lower than that in the control group, which could be reversed by nesfatin-1 treatment (Fig. 7E, G). In contrast, the ASIC1a expression in the chondrocytes of the model group was significantly higher than that in the control group, which could be reversed by nesfatin-1 treatment (Fig. 7F, H).

As shown in Fig. 7I–K, the serum levels of inflammatory cytokines, including IL-6, IL-1β, and TNF-α, were significantly increased in the model group than those in the control group, which could be reversed by nesfatin-1 treatment.

DISCUSSION

In the present study, we found that nesfatin-1 attenuated acidosis-induced cytotoxicity and intracellular Ca^{2+} elevation in chondrocytes. Moreover, acid-induced oxidative stress, inflammation, and apoptosis in chondrocytes were ameliorated by nesfatin-1 treatment, which is similar to the effect of the ASIC1a-specific blocker PcTx1. Nesfatin-1 decreased the overexpression of ASIC1a protein in acid-stimulated chondrocytes via the ERK1/2/NF-κB signaling pathway. Furthermore, nesfatin-1 treatment markedly ameliorated the clinical signs and cartilage degradation and decreased ASIC1a protein levels in the chondrocytes of rats with AA. Collectively, these results indicate that nesfatin-1 exerts antioxidant, anti-inflammatory, and antiapoptotic effects on acidosis-stimulated chondrocytes and alleviates arthritis

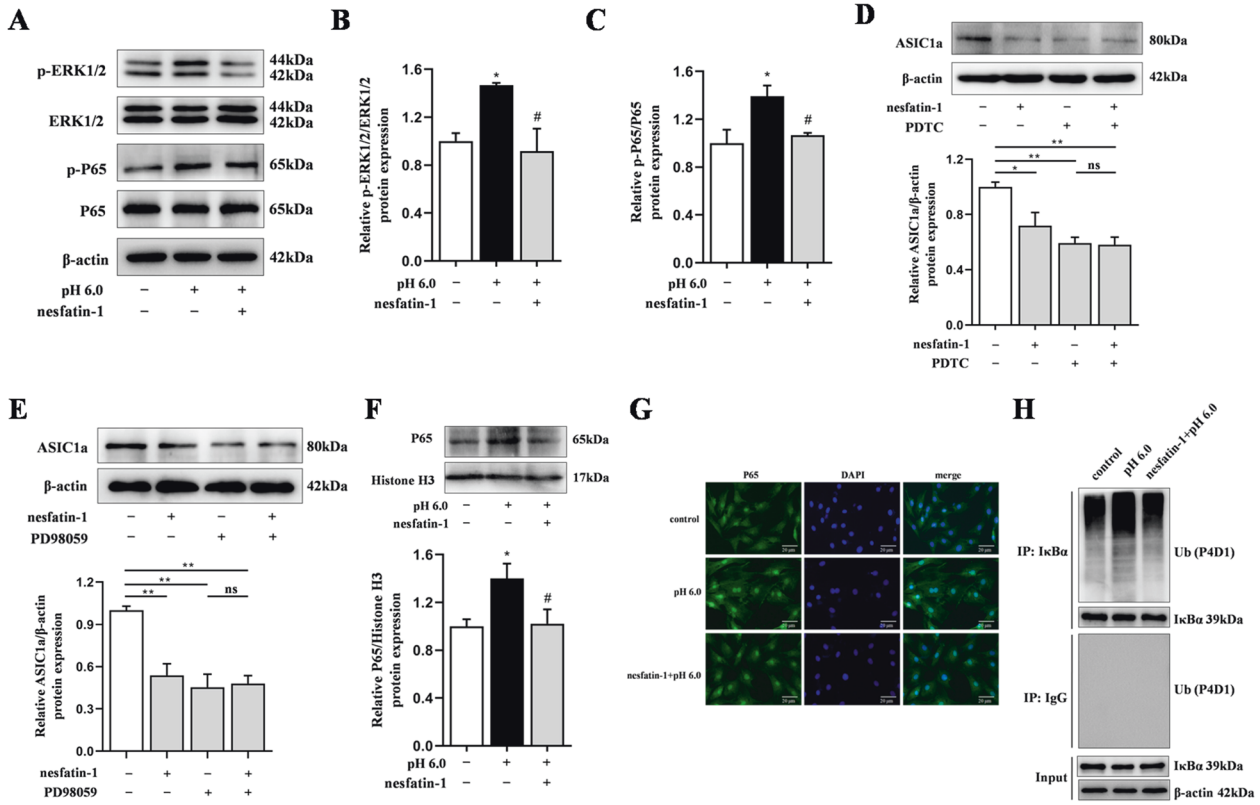

Fig. 6 Nesfatin-1 reduced ASIC1a expression via the acidosis-induced activation of the MAPK/ERK1/2 and NF-κB signaling pathways in articular chondrocytes. A–**C** The p-ERK1/2/ERK1/2 and p-P65/P65 protein levels in acid-mediated chondrocytes after nesfatin-1 pretreatment were measured by western blotting. **D** The ASIC1a protein levels after nesfatin-1 and PDTC pretreatment were measured by western blotting. **E** The ASIC1a protein levels after nesfatin-1 and PD098059 pretreatment were measured using western blotting. **F** The P65/histone H3 protein levels after nesfatin-1 treatment were measured by western blotting in acid-mediated chondrocytes. **G** Immunocytochemical images of NF-κB P65, showing its expression and nuclear translocation in acid-mediated chondrocytes treated with nesfatin-1. **H** Effects of nesfatin-1 on IκBα ubiquitination in acid-mediated chondrocytes treated with nesfatin-1. Data represent the mean ± SEM values for three independent experiments. $^{*}P < 0.05$, $^{**}P < 0.01$ compared to the control group; $^{\#}P < 0.05$ compared to the pH 6.0 group; ns no significance.

symptoms in rats with AA via ERK1/2/NF-κB-dependent decreases in ASIC1a channel expression (Fig. 8).

Extracellular acidosis has been noted at sites of ischemia, inflammation, and hypoxia[35,36]. As RA is a chronic inflammatory disease, the pH value of the articular SF may drop to 6.0[15,16]. Furthermore, low SF pH is reportedly related to radiological joint destruction in patients with RA[17] and affect cartilage homeostasis[37]. Considering the findings of the abovementioned studies and the fact that chondrocytes, the only cell type found in articular cartilage, are crucial in the pathogenesis of arthritis and are significantly affected by local pH[38], acid-stimulated chondrocytes have been widely used as a cell model to investigate the pathogenesis of RA[18,28,39,40]. Rats with AA are experimental animal models of polyarthritis and are widely used to mimic human RA and explore the pathophysiology of RA[41]. The articular SF of rats with AA has been found to have lower pH than that of rats without AA[18]. Considering that AA causes considerable systemic inflammation that results in severe joint swelling and remodeling, this animal model was selected for the present study. However, this model mainly involves inflammation in the articulation and focuses on chondrocyte pathophysiology, while excluding the autoimmune spectrum of RA. Since RA is an autoimmune disease, autoimmunity-based RA models, such as collagen-induced arthritis (CIA) or K/BxN mouse models, should be used in further research to evaluate the therapeutic effect of nesfatin-1 on RA disease.

PcTx1, a peptide isolated from the venom of the southern spider tarantula *Psalmopoeus cambridgei*, can specifically and strongly inhibit the current mediated by homomeric ASIC1a[42]. Research on chimeras indicates that PcTx1 principally binds to both cysteine-rich domains I and II (CRDI and CRDII, respectively) of the extracellular loop of ASIC1a. Moreover, numerous studies have indicated that PcTx1 can block the ASIC1a channel in articular chondrocytes and alleviate arthritis symptoms in rats with AA[34,43]. Therefore, PcTx1 was selected as a positive control drug in this study. MTX, a traditional DMARD with folate antagonist and anti-inflammatory activity, is the cornerstone of RA treatment[44]. MTX exerts anti-inflammatory and protective effects against joint damage, including cartilage and bone erosion, cellular infiltration, and synovial proliferation, in rats with AA[45,46]. Therefore, MTX was used as the other positive control drug.

Several lines of evidence have confirmed the anti-inflammatory, antiapoptotic, and antioxidant effects of nesfatin-1. Recent studies have suggested that nesfatin-1 attenuates myocardial infarction injury by targeting inflammation[47]. Moreover, it attenuates tubular apoptosis by preventing caspase-3 activity[48] and is reported to promote trophoblast cell proliferation by inhibiting oxidative stress[49]. Thus, these protective effects of nesfatin-1 indicate that it may protect acid-stimulated chondrocytes and improve the symptoms of arthritis in rats with AA. The KEGG enrichment pathway analyses showed that mRNAs differentially expressed between the nesfatin-1 group and the pH 6.0 group were involved in pathways related to oxidative stress, inflammation, and apoptosis. Therefore, to analyze the protective effect of nesfatin-1 on acid-stimulated chondrocytes, we focused on its

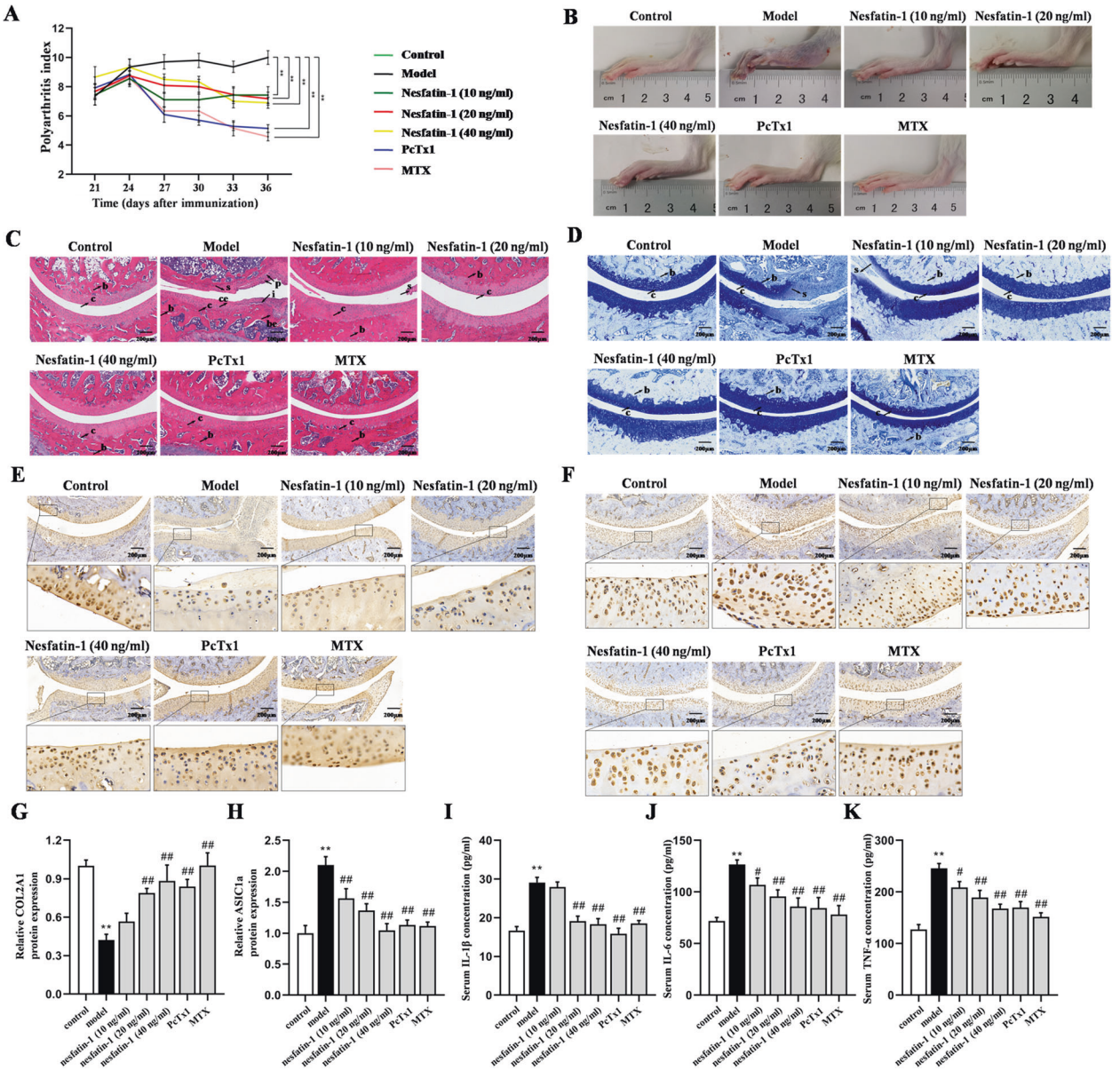

Fig. 7 Nesfatin-1 treatment attenuated clinical signs, improved the histopathological features of arthritic joints, and reduced the serum inflammatory cytokine levels and COL2A1 and ASIC1a expression levels in the chondrocytes of rats with AA. A Effects of nesfatin-1 on the polyarthritis index of rats with AA. **B** Photographs of representative paws from each group. **C** Representative micrographs of HE-stained histological sections of the joints, showing bone (b), bone erosion (be), cartilage (c), cartilage erosion (ce), synovium (s), inflammatory cells (i), and pannus formation (P). **D** Representative micrographs of toluidine blue-stained histological sections of the joints, showing bone (b), cartilage (c), and synovium (s). **E**, **G** Representative micrographs and quantitative analysis of immunohistochemical detection of COL2A1 expression. **F**, **H** Representative micrographs and quantitative analysis of immunohistochemical detection of ASIC1a expression. **I**–**K** The serum IL-6, IL-1β, and TNF-α levels were measured by ELISA assay. **A** $^{**}P < 0.01$ compared to model group ($n = 8$–10 per group). **G**–**K** $^{**}P < 0.01$ compared to the control group; $^{\#}P < 0.05$, $^{\#\#}P < 0.01$ compared to model group ($n = 8$–10 per group).

anti-inflammatory, antiapoptotic, and antioxidant properties in the subsequent experiments. We found that nesfatin-1 treatment decreased the increased levels of oxidative stress, inflammation, and apoptosis induced by acid stimulation in chondrocytes, indicating a protective effect of nesfatin-1 on cartilage and its therapeutic potential for RA. Additionally, nesfatin-1 has been reported to play an important role in glucose homeostasis, lipid metabolism, modulation of gastrointestinal functions, cardiovascular, and reproductive functions[9]. These diverse effects may cause a variety of side effects in the use of nesfatin-1. However, in the present study, nesfatin-1 was injected locally in the joint cavity. Local application of nesfatin-1 has potential advantages compared to systemic administration, including the use of smaller dosages to reduce side effects and potential toxicity. In the current study, no obvious side effects were observed throughout the whole experiment, suggesting that nesfatin-1 exhibits a good safety profile on topical application. Further research is needed to establish more detailed information about the possible side effect following the systemic administration of nesfatin-1.

ASIC1a is involved in several acidosis-related pathophysiological processes, including RA. We previously showed that ASIC1a-contributes to acidosis-induced chondrocyte damage[50]. More

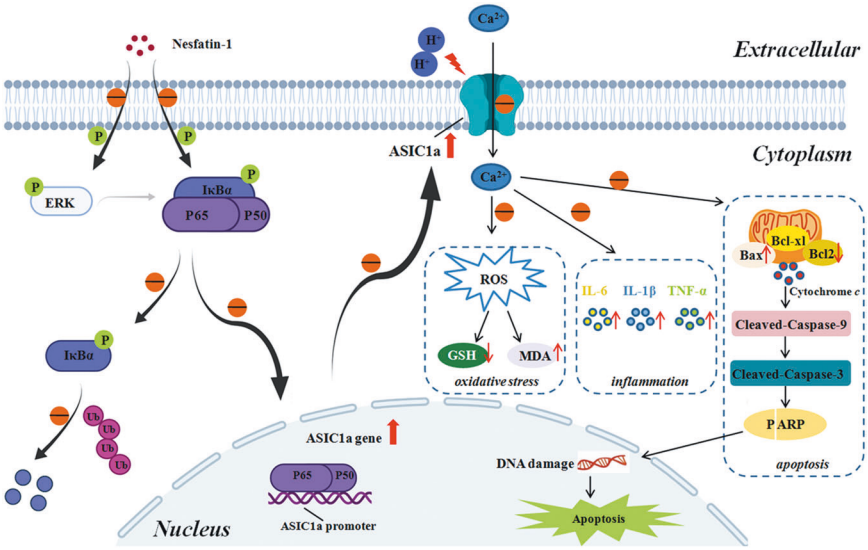

Fig. 8 Mechanism schematic presentation that nesfatin-1 exerts antioxidant, anti-inflammatory, and antiapoptotic effects on acidosis-stimulated chondrocytes via inhibition of ASIC1a expression. Nesfatin-1 decreased the phosphorylation of ERK1/2, ubiquitination and degradation of IκBα, and nuclear translocation of NF-κB P65, leading to downregulation of ASIC1a expression. Acid-induced $(Ca^{2+})i$ elevation was suppressed, andoxidative stress, inflammation, and apoptosis were inhibited.

recently, ASIC1a expression was found to significantly increase in the articular cartilage of rats with AA[28]. Treatment with the ASIC1a-specific blocker PcTx1 was found to reverse the extracellular acidosis-induced death of chondrocytes and ameliorate disease severity in rats with AA[23,51]. Consistent with these findings, the results of the present study further confirmed that PcTx1 can reduce acid-stimulated chondrocyte apoptosis and decrease articular cartilage destruction in rats with AA. Moreover, nesfatin-1 showed a protective effect similar to that of PcTx1. Combined treatment with nesfatin-1 and PcTx1 did not provide additional protection beyond that obtained with PcTx1 alone, suggesting that there is no synergy between nesfatin-1 and PcTx1, and inhibiting ASIC1a channel is likely involved in nesfatin-1-mediated protection. Therefore, the effect of nesfatin-1 on ASIC1a channel function and expression was further investigated. Our current study showed that nesfatin-1 treatment decreased the increased ASIC1a protein levels in acid-stimulated chondrocytes. Ca^{2+} is believed to be a crucial downstream mediator effector after ASIC1a channel activation, and extracellular acidosis could activate ASIC1a, ultimately contributing to acid-induced articular chondrocyte injury via $(Ca^{2+})i$ overload. The current study confirmed that nesfatin-1 could downregulate the increased $(Ca^{2+})i$ in acid-stimulated articular chondrocytes. These data suggest that nesfatin-1 treatment would provide a novel strategy for RA therapy by reducing cartilage destruction via decrease in ASIC1a protein levels and $(Ca^{2+})i$.

NF-κB, an evolutionarily conserved transcription factor, plays a critical role in inducing the expression of genes involved in various biological processes[52]. Accumulating evidence suggests that NF-κB activation is involved in ASIC1a protein synthesis. Increasing number of research studies have shown that IL-1β and TNF-α can enhance the activity of the ASIC1a gene promoter by increasing the DNA-binding activity of NF-κB, which could be inhibited by PDTC, an NF-κB inhibitor[18]. Considering that nesfatin-1 mainly exerts anti-inflammatory effects in various diseases by inhibiting the NF-κB signaling pathway[9], the possibility of involvement of the NF-κB signaling pathway in the regulation of ASIC1a expression by nesfatin-1 was investigated. Our results indicated that nesfatin-1 could inhibit the overexpression of p-P65/P65, degradation of ubiquitylated IκBα, and nuclear translocation of NF-κB P65 in acid-stimulated chondrocytes.

The MAPK/ERK signaling pathway, a protein serine/threonine kinase cascade[53], participates in various biological processes. We previously showed that the upregulation of ASIC1a expression by proinflammatory cytokines could be partially abrogated by PD098059, an ERK1/2 inhibitor[18], suggesting that ERK1/2 activation is involved in the proinflammatory cytokine-induced upregulation of ASIC1a expression. Consistent with these findings, in the current study, combined treatment with nesfatin-1 and PD098059 did not lead to additional decreases beyond those obtained with PD098059 alone, suggesting that MAPK/ERK signaling is likely involved in nesfatin-1-mediated inhibition of ASIC1a production.

In conclusion, the present study showed that the antioxidant, anti-inflammatory, and antiapoptotic effects of nesfatin-1 on acid-stimulated chondrocytes are, at least partially, mediated by the decrease inASIC1a expression and function via MAPK/ERK and NF-κB signaling pathways. Our findings highlight a novel mechanism underlying the protective effect of nesfatin-1 and suggest potential future therapeutic strategies for RA.

DATA AVAILABILITY

The data sets used during the current study are available from the corresponding author on reasonable request.

REFERENCES

1. Gibofsky, A. Epidemiology, pathophysiology, and diagnosis of rheumatoid arthritis: a synopsis. *Am. J. Manag. Care* **20**, S128–S135 (2014).
2. Aletaha, D. & Smolen, J. Diagnosis and management of rheumatoid arthritis: a review. *JAMA* **320**, 1360–1372 (2018).
3. Yu, H., Hsiung, N., Chiang, J. & Shen, H. The risk of coronary artery disease in patients with rheumatoid arthritis using Chinese herbal products and conventional medicine in parallel: a population-based cohort study. *BMC Complement. Med. Ther.* **20**, 100 (2020).
4. Plant, M., Saklatvala, J., Borg, A., Jones, P. & Dawes, P. Measurement and prediction of radiological progression in early rheumatoid arthritis. *J. Rheumatol.* **21**, 1808–1813 (1994).
5. Kim, H. & Song, Y. Apoptotic chondrocyte death in rheumatoid arthritis. *Arthritis. Rheum.* **42**, 1528–1537 (1999).
6. Rezaei, H. et al. In early rheumatoid arthritis, patients with a good initial response to methotrexate have excellent 2-year clinical outcomes, but radiological

progression is not fully prevented: data from the methotrexate responders population in the SWEFOT trial. *Ann. Rheum. Dis.* **71**, 186–191 (2012).
7. Scott, D., Wolfe, F. & Huizinga, T. Rheumatoid arthritis. *Lancet* **376**, 1094–1108 (2010).
8. Oh-I, S. et al. Identification of nesfatin-1 as a satiety molecule in the hypothalamus. *Nature* **443**, 709–712 (2006).
9. Xu, Y. & Chen, F. Antioxidant, anti-inflammatory and anti-apoptotic activities of nesfatin-1: a review. *J. Inflamm. Res.* **13**, 607–617 (2020).
10. Nazarnezhad, S. et al. Nesfatin-1 protects PC12 cells against high glucose-induced cytotoxicity via inhibiting oxidative stress, autophagy and apoptosis. *Neurotoxicology* **74**, 196–202 (2019).
11. Tasatargil, A. et al. Cardioprotective effect of nesfatin-1 against isoproterenol-induced myocardial infarction in rats: Role of the Akt/GSK-3β pathway. *Peptides* **95**, 1–9 (2017).
12. Jiang, L. et al. Nesfatin-1 suppresses interleukin-1β-induced inflammation, apoptosis, and cartilage matrix destruction in chondrocytes and ameliorates osteoarthritis in rats. *Aging* **12**, 1760–1777 (2020).
13. Xu, Y. & Chen, F. Acid-sensing ion channel-1a in articular chondrocytes and synovial fibroblasts: a novel therapeutic target for rheumatoid arthritis. *Front. Immunol.* **11**, 580936 (2020).
14. Wemmie, J. A., Taugher, R. J. & Kreple, C. J. Acid-sensing ion channels in pain and disease. *Nat. Rev. Neurosci.* **14**, 461–471 (2013).
15. Cummings, N. A. & Nordby, G. L. Measurement of synovial fluid pH in normal and arthritic knees. *Arthritis. Rheum.* **9**, 47–56 (1966).
16. Farr, M., Garvey, K., Bold, A. M., Kendall, M. J. & Bacon, P. A. Significance of the hydrogen ion concentration in synovial fluid in rheumatoid arthritis. *Clin. Exp. Rheumatol.* **3**, 99–104 (1985).
17. Geborek, P., Saxne, T., Pettersson, H. & Wollheim, F. A. Synovial fluid acidosis correlates with radiological joint destruction in rheumatoid arthritis knee joints. *J. Rheumatol.* **16**, 468–472 (1989).
18. Zhou, R. P. et al. Interleukin-1beta and tumor necrosis factor-alpha augment acidosis-induced rat articular chondrocyte apoptosis via nuclear factor-kappaB-dependent upregulation of ASIC1a channel. *Biochim. Biophys. Acta Mol. Basis Dis.* **1864**, 162–177 (2018).
19. Yuan, F. L. et al. Acid-sensing ion channel 1a mediates acid-induced increases in intracellular calcium in rat articular chondrocytes. *Mol. Cell Biochem.* **340**, 153–159 (2010).
20. Zu, S. Q. et al. Acid-sensing ion channel 1a mediates acid-induced pyroptosis through calpain-2/calcineurin pathway in rat articular chondrocytes. *Cell Biol. Int.* **44**, 2140–2152 (2020).
21. Rong, C. et al. Inhibition of acid-sensing ion channels by amiloride protects rat articular chondrocytes from acid-induced apoptosis via a mitochondrial-mediated pathway. *Cell Biol. Int.* **36**, 635–641 (2012).
22. Hu, W. et al. Blockade of acid-sensing ion channels protects articular chondrocytes from acid-induced apoptotic injury. *Inflamm. Res.* **61**, 327–335 (2012).
23. Zhang, Y. et al. ASIC1a induces synovial inflammation via the Ca/NFATc3/RANTES pathway. *Theranostics* **10**, 247–264 (2020).
24. Niu, R. et al. ASIC1a promotes synovial invasion of rheumatoid arthritis via Ca/Rac1 pathway. *Int. Immunopharmacol.* **79**, 106089 (2020).
25. Wang, Z. et al. Nesfatin-1 alleviates acute lung injury through reducing inflammation and oxidative stress via the regulation of HMGB1. *Eur. Rev. Med. Pharmacol. Sci.* **24**, 5071–5081 (2020).
26. Tang, C., Fu, X., Xu, X., Wei, X. & Pan, H. The anti-inflammatory and anti-apoptotic effects of nesfatin-1 in the traumatic rat brain. *Peptides* **36**, 39–45 (2012).
27. Karadeniz Cerit, K. et al. Nesfatin-1 ameliorates oxidative bowel injury in rats with necrotizing enterocolitis: The role of the microbiota composition and claudin-3 expression. *J. Pediatr. Surg.* **55**, 2797–2810 (2020).
28. Zhou, R., Wu, X., Wang, Z., Ge, J. & Chen, F. Interleukin-6 enhances acid-induced apoptosis via upregulating acid-sensing ion channel 1a expression and function in rat articular chondrocytes. *Int. Immunopharmacol.* **29**, 748–760 (2015).
29. Wei, X. et al. Nerve growth factor promotes ASIC1a expression via the NF-κB pathway and enhances acid-induced chondrocyte apoptosis. *Int. Immunopharmacol.* **82**, 106340 (2020).
30. Zhang, L., Leng, T., Yang, T., Li, J. & Xiong, Z. Protein kinase C regulates ASIC1a protein expression and channel function via NF-kB signaling pathway. *Mol. Neurobiol.* **57**, 4754–4766 (2020).
31. Nie, F. et al. Reactive oxygen species accumulation contributes to gambogic acid-induced apoptosis in human hepatoma SMMC-7721 cells. *Toxicology* **260**, 60–67 (2009).
32. Xu, Y. & Chen, F. Factors and molecular mechanisms influencing the protein synthesis, degradation and membrane trafficking of ASIC1a. *Front. Cell Dev. Biol.* **8**, 596304 (2020).
33. Xiong, Z. G. et al. Neuroprotection in ischemia: blocking calcium-permeable acid-sensing ion channels. *Cell* **118**, 687–698 (2004).
34. Wu, X., Ren, G., Zhou, R., Ge, J. & Chen, F. The role of Ca in acid-sensing ion channel 1a-mediated chondrocyte pyroptosis in rat adjuvant arthritis. *Lab. Invest.* **99**, 499–513 (2019).
35. Yuan, F. L. et al. Molecular actions of ovarian cancer G protein-coupled receptor 1 caused by extracellular acidification in bone. *Int. J. Mol. Sci.* **15**, 22365–22373 (2014).
36. Rajamäki, K. et al. Extracellular acidosis is a novel danger signal alerting innate immunity via the NLRP3 inflammasome. *J. Biol. Chem.* **288**, 13410–13419 (2013).
37. Arnett, T. Acidosis, hypoxia and bone. *Arch. Biochem. Biophys.* **503**, 103–109 (2010).
38. Chang, J. et al. The dual role of autophagy in chondrocyte responses in the pathogenesis of articular cartilage degeneration in osteoarthritis. *Int. J. Mol. Med.* **32**, 1311–1318 (2013).
39. Chen, Y. et al. Necrostatin-1 ameliorates adjuvant arthritis rat articular chondrocyte injury via inhibiting ASIC1a-mediated necroptosis. *Biochem. Biophys. Res. Commun.* **504**, 843–850 (2018).
40. Gao, W., Xu, Y., Ge, J. & Chen, F. Inhibition of acid-sensing ion channel 1a attenuates acid-induced activation of autophagy via a calcium signaling pathway in articular chondrocytes. *Int. J. Mol. Med.* **43**, 1778–1788 (2019).
41. Kim, W. et al. Evaluation of anti-inflammatory potential of the new ganghwaljetongyeum on adjuvant-induced inflammatory arthritis in rats. *Evid. Based Complement. Alternat. Med.* **2016**, 1230294 (2016).
42. Chen, X., Kalbacher, H. & Gründer, S. The tarantula toxin psalmotoxin 1 inhibits acid-sensing ion channel (ASIC) 1a by increasing its apparent H+ affinity. *J. Gen. Physiol.* **126**, 71–79 (2005).
43. Dai, B. et al. ASIC1a promotes acid-induced autophagy in rat articular chondrocytes through the AMPK/FoxO3a pathway. *Int. J. Mol. Sci.* **18**, 2125 (2017).
44. Dudics, S. et al. Natural products for the treatment of autoimmune arthritis: their mechanisms of action, targeted delivery, and interplay with the host microbiome. *Int. J. Mol. Sci.* **19**, 2508 (2018).
45. Chang, Y. et al. CP-25, a novel compound, protects against autoimmune arthritis by modulating immune mediators of inflammation and bone damage. *Sci. Rep.* **6**, 26239 (2016).
46. Asenso, J. et al. Methotrexate improves the anti-arthritic effects of Paeoniflorin-6′-O-benzene sulfonate by enhancing its pharmacokinetic properties in adjuvant-induced arthritis rats. *Biomed. Pharmacother.* **112**, 108644 (2019).
47. Naseroleslami, M., Sharifi, M., Rakhshan, K., Mokhtari, B. & Aboutaleb, N. Nesfatin-1 attenuates injury in a rat model of myocardial infarction by targeting autophagy, inflammation, and apoptosis. *Arch. Physiol. Biochem.* 1–9 https://doi.org/10.1080/13813455.2020.1802486. (2020). Online ahead of print.
48. Jiang, G. et al. The protective effect of nesfatin-1 against renal ischemia-reperfusion injury in rats. *Ren. Fail.* **37**, 882–889 (2015).
49. Li, T., Wei, S., Fan, C., Tang, D. & Luo, D. Nesfatin-1 Promotes Proliferation, Migration and Invasion of HTR-8/SVneo Trophoblast Cells and Inhibits Oxidative Stress via Activation of PI3K/AKT/mTOR and AKT/GSK3β Pathway. *Reprod. Sci.* **28**, 550–561 (2021).
50. Yuan, F. L. et al. Inhibition of acid-sensing ion channels in articular chondrocytes by amiloride attenuates articular cartilage destruction in rats with adjuvant arthritis. *Inflamm Res.* **59**, 939–947 (2010).
51. Song, S. J. et al. 17β-estradiol attenuates rat articular chondrocyte injury by targeting ASIC1a-mediated apoptosis. *Mol Cell Endocrinol* **505**, 110742 (2020).
52. Mitchell, J. & Carmody, R. NF-κB and the Transcriptional Control of Inflammation. *Int Rev Cell Mol Biol.* **335**, 41–84 (2018).
53. Roskoski, R. ERK1/2 MAP kinases: structure, function, and regulation. *Pharmacol Res.* **66**, 105–143 (2012).

ACKNOWLEDGEMENTS

This work was supported by the National Natural Science Foundation of China (Grant Number 81873986).

AUTHOR CONTRIBUTIONS

All authors have participated in drafting the paper and approved the final version to be published. F.H. Chen and Y.Y. Xu took the responsibility for study design. Y.Y. Xu, Z.Y. Zai, T. Zhang, L.F. Wang, X.W. Qian, D.D. Xu, J.J. Tao, Z. Lu and X.Q. Peng performed the experiments, data acquisition, and the data analysis. Y.Y. Xu took the responsibility for interpretation of the data.

COMPETING INTERESTS

The authors declare no competing interests.

ETHICS APPROVAL

Ethical protocols (No. LLSC20180328) approved by the Ethics Committee of Anhui Medical University. This study was performed in accordance with the Declaration of Helsinki.

ADDITIONAL INFORMATION

Supplementary information The online version contains supplementary material available at https://doi.org/10.1038/s41374-022-00774-y.

Correspondence and requests for materials should be addressed to Feihu Chen.